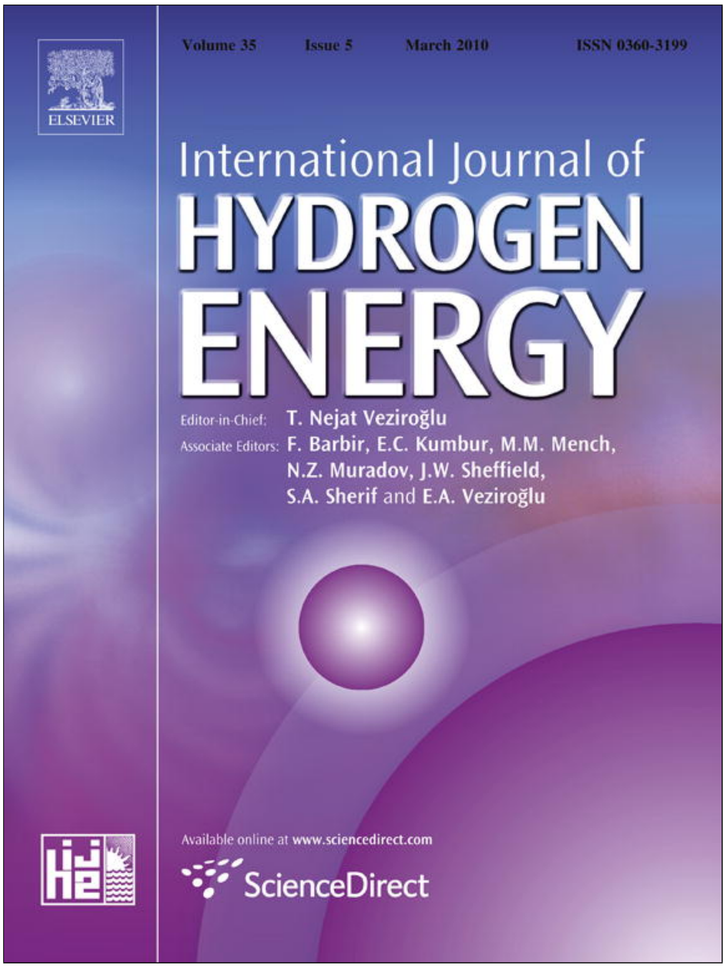

INTERNATIONAL JOURNAL OF HYDROGEN ENERGY 35 (2010) 2018–2024

Available at www.sciencedirect.com

journal homepage: www.elsevier.com/locate/he

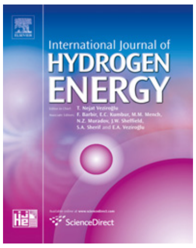

Methanol oxidation on carbon supported Pt–Ru catalysts prepared by electrodeposition – Evaluation of Nafion® 117 film effect

J.M. Sieben [a,*], M.M.E. Duarte [a,b], C.E. Mayer [a,b]

[a] Instituto de Ingeniería Electroquímica y Corrosión (INIEC), Universidad Nacional del Sur, Av. Alem 1253, (B8000CPB) Bahía Blanca, Buenos Aires, Argentina
[b] Comisión de Investigaciones Científicas de la Provincia de Buenos Aires (CIC), Argentina

ARTICLE INFO

Article history:
Received 25 November 2009
Accepted 16 December 2009
Available online 20 January 2010

Keywords:
Electrodeposited Pt–Ru supported catalysts
Nafion films
Methanol oxidation

ABSTRACT

Diverse electrochemical techniques were performed in order to obtain meaningful information about the methanol oxidation reaction on nanostructured planar carbon supported Pt–Ru electrodes prepared by electrodeposition, on which a layer of Nafion ionomer was incorporated. A metallic deposit consisting of dendritic agglomerates (between 50 and 200 nm) constituted by smaller particles (6 nm) was obtained. The average bulk Ru content obtained by EDX analysis was between 23 and 25 at. %. A decrease of the activity in the electrodes for methanol oxidation was determined when the thickness of the Nafion 117 film was increased. These results may be associated with the partial blocking of the surface active sites by hydrophobic domains of the polymer, and the presence of CO_2 molecules retained within the Nafion hydrophilic microchannels. EIS results indicated that methanol electro-oxidation mechanism does not change with Nafion presence.

1. Introduction

In typical manufacturing methods of anodes for DMFCs the utilization of noble metal catalyst is inefficient, due to agglomeration of catalyst powders and lack of contact between Pt–Ru particles and the polymeric electrolyte [1].

One approach to avoid these difficulties is preparing Pt–Ru electrodes by electrodeposition over carbon substrates in an aqueous solution. Selective deposition of catalyst particles at desirable locations with both ionic and electronic accessibility is achieved.

One aspect that must be taken into account is the effect of the ionomer that act as both proton conductor and binder [2]. In proton exchange membranes fuel cells, Nafion commercial perfluorinated ionic polymers are the most used due to its excellent proton conductivity, thermal and chemical stability, and mechanical strength [3].

The use of planar nanostructured electrodes provides a useful tool for studying the electrokinetics and mass-transport of electrochemical reactions at a catalyst on which a thin layer of a polymeric conductive electrolyte has been placed. These electrodes are composed of a high surface area nanostructured catalyst electrodeposited on a non-porous conductive substrate. With this arrangement, the effect of a porous structure is avoided although retaining the characteristics of a dispersed catalyst. This is a convenient approach to the investigation of methanol oxidation at the interface between a real electrocatalyst and a solid polymer electrolyte membrane.

The aim of the present work is to prepare planar supported Pt–Ru electrodes by successive cycles of potentiostatic pulses

---

[*] *Corresponding author*. Tel.:/fax: +54 291 4595182.
E-mail address: jmsieben@uns.edu.ar (J.M. Sieben).

doi:10.1016/j.ijhydene.2009.12.078

to use in methanol oxidation, and to study the effect of Nafion films deposited over the catalyst.

2. Experimental

Glassy carbon (GC) discs of 0.07 cm^2 exposed geometric area were used as catalyst support.

Nafion® 117 films of diverse thickness were prepared spraying different amounts of an ionomeric solution (5 wt. %) over Pt–Ru/GC electrodes, followed by drying in air for a day before use. The characteristics of the polymeric films are summarized in Table 1.

Electrochemical measurements were carried out in a conventional three-compartment glass cell at temperatures between 25 °C and 60 °C. The counter-electrode was a platinum sheet, and a saturated calomel electrode (SCE) served as the reference. All potentials mentioned in this work are referred to this electrode. An inert nitrogen atmosphere was maintained over the electrolyte. A PAR 273 and a Voltalab PGZ-301 were used to run the experiments. Electrochemical techniques such as EIS, cyclic voltammetry, linear sweep voltammetry and chronoamperometry were used to characterize the catalysts and to study the methanol oxidation kinetics. The impedance measurements were done in the frequency range from 100 kHz to 10 mHz by applying a sine wave of 10 mV amplitude.

The catalysts were synthesized by electrodeposition at 25 °C using a diluted solution of platinum and ruthenium salts (2 mM H_2PtCl_6 + 2 mM $RuCl_3$ in 0.5 M H_2SO_4). The electrodeposition was carried out using multiple successive potentiostatic pulses ($E_{cathodic} = -0.5$ V $t_{cathodic} = 30$ s, $E_{anodic} = 1$ V $t_{anodic} = 5$ s) by applying 30 consecutives cycles. After deposition, the electrodes were thoroughly rinsed with bidistilled water and tested in sulfuric acid solution by cyclic voltammetry at a rate of 50 mV s^{-1}.

The active surface area of the electrocatalysts was determined by copper underpotential deposition (Cu-UPD). Experimental details were described in a previous paper [4].

The electrodes activity for methanol oxidation was measured in 1 M CH_3OH + 0.5 M H_2SO_4 solution by applying a potential sweep at a scan rate of 50 mV s^{-1}. Chronoamperometry curves were obtained at different potentials, applying potentials pulses from an initial potential of 0 V. Current densities for methanol oxidation were normalized to the active surface area.

The morphology of the catalyst surface and the particle size were analyzed using SEM microscopy. Bulk composition analysis of Pt–Ru catalysts was performed using EDX analysis. In addition, the structure of the electrodes was characterized by XRD.

Table 1 – Characteristics of Nafion® 117 layer.

V_{Nafion}/μL	W/A_g mg cm^{-2}	l_{dry}/μm
1	0.621	0.85 ± 0.30
5	3.107	5.10 ± 0.40
10	6.214	9.72 ± 0.43

W: weight of Nafion® 117 film, l_{dry}: thickness of dry Nafion® 117 film, A_g: geometric area.

3. Results and discussion

3.1. Characterization of supported Pt–Ru catalysts

Ru contents between 23 and 25 at. % were measured by EDX in all the analyzed samples. The proportion of deposited ruthenium to platinum is in the expected order, taking into account that the mol ratio of $RuCl_3$ concentration to H_2PtCl_6 concentration is equal to one [4].

A SEM micrograph of Pt–Ru catalyst on glassy carbon is shown in Fig. 1. The electrodeposition method here used generates rough islands with incipient dendrites. The dendritic shape of the islands appears when the deposition process occurs under mass-transfer or mixed control conditions [5]. The dendrites growth is accelerated due to a faster diffusion rate of the metal ions at the tips of the excrescences. Furthermore, another plausible explanation suggests that crystallite tips formation is a probable consequence of the interplay of primary and secondary nucleation [6]. The result of secondary nucleation is formation of complex micro and nanograined Pt structures. Moreover, surface formation of particle agglomerates may also occur through migration and coalescence of Pt–Ru nanoparticles favored by weak interaction of metals with GC substrate (surface diffusion sticking process) [7]. In fact both processes can contribute to the catalyst morphology observed in SEM image.

Debye–Scherrer's equation was used to estimate the average Pt–Ru crystallite. The average size of the crystallite measured by XRD is around 6 nm. This means that Pt–Ru particles determined by SEM microscopy are, in fact, agglomerates comprising much smaller particles. The XRD patterns (Fig. 2) indicate that Ru was dissolved into the fcc lattice of Pt, forming an alloy where a Pt atom is exchanged by one of Ru. The Pt–Ru/GC-10 catalyst preserved the fcc Pt lattice structure, with a slight shift of Pt diffraction peaks. Typical peaks of the crystalline face centered cubic Pt (111), (200) and (220) planes were visible.

Cyclic voltammograms of Pt–Ru catalysts with different Nafion film thickness in absence of methanol are shown in Fig. 3. The coulombic charge related to the hydrogen adsorption/desorption processes decreases when Nafion film thickness increases. The perfluorocarbon backbone can partially block the electrochemical active sites in the catalyst surface by the formation of hydrophobic domains that hinder the proton access to the electrode surface [8].

In addition, when the electrode is covered by the ionomeric film the extent to which the Nafion penetrates the mesoporous structure of the supported catalyst is unknown. The Nafion solution wets the mesoporous structure of the electrode inefficiently, so the incomplete penetration (compared to the electrode without Nafion) might contribute to decrease hydrogen adsorption over the Pt atoms.

3.2. Methanol oxidation on bare Pt–Ru and Pt–Ru covered by Nafion

Fig. 4 shows the cyclic voltammetry curves recorded for Nafion/Pt–Ru/GC electrodes at temperatures between 25 °C and 60 °C at 50 mV s^{-1}. At 25 °C the onset of methanol

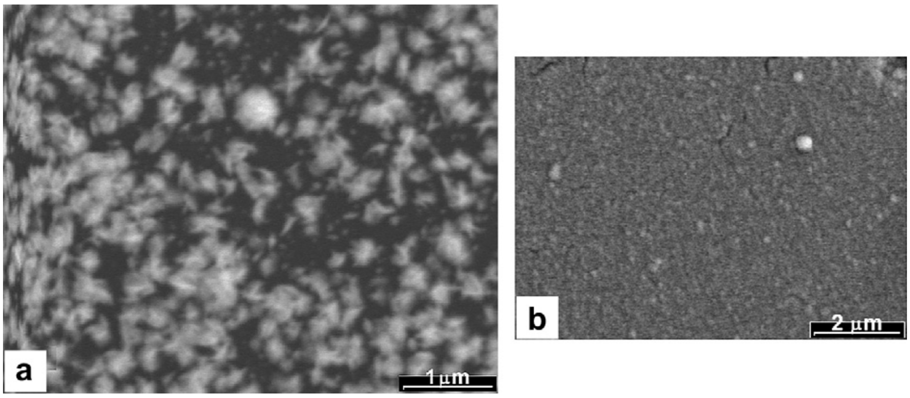

Fig. 1 – SEM image of a Pt–Ru/GC catalyst (a). SEM image showing a Nafion® 117 film over a supported Pt–Ru catalyst (b).

oxidation takes place at 0.35 V, and shift to lower potentials with increasing temperature, falling to 0.2 V at 60 °C. In addition, the electrode performance for methanol oxidation, taken from the current peak, increases more than ten times when the temperature is raised from 25 °C to 60 °C. The desorption rate of the adsorbed residues increases with temperature because the adsorption energy decreases, resulting in weakly adsorbed and more reactive CO_{ads} molecules. Moreover, the methanol diffusion rate increases with temperature.

The presence of a Nafion film reduces the electrode activity for methanol oxidation (Fig. 4). This significant diminution can be associated with a reduction of the available active sites for the reaction and the inefficiently penetration of the polymer in the catalyst structure, as was commented previously. Furthermore, the polymer presence in a planar electrode may also retard the CO_2 removal from the active reaction sites. This can result in entrapment of the gas inside the polymeric layer and blocking of the microchannels in the structure, limiting the arrival of the reactant to the catalyst surface.

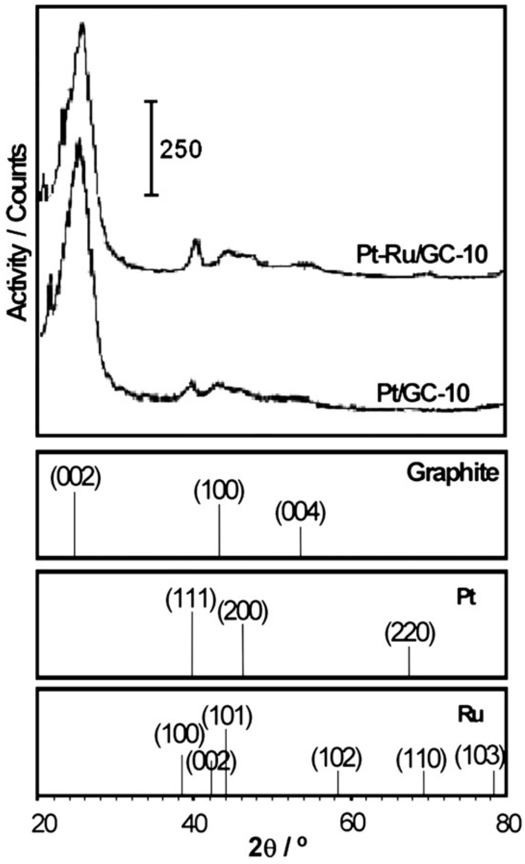

Fig. 2 – XRD spectra of the systems Pt/GC and Pt–Ru/GC.

Fig. 5 shows the Tafel plots obtained from stationary polarization experiments in 1 M CH_3OH + 0.5 M H_2SO_4 solutions at room temperature for different Nafion thicknesses. The slopes were obtained in the potential region in which the studied systems obey a Tafel-type behavior. Slopes ranging from 115 to 125 mV dec^{-1} in agree with that reported in literature [4,9,10] were determined with a reasonable level of accuracy. Additionally, the potentiostatic tests show that methanol oxidation is not limited by mass-transfer polarization as was presented in a detailed analysis by Vidaković et al. [10] and Zecevic et al. [11].

The Tafel slope behavior indicates that the rate-determining step (rds) involves the desorptive oxidation of CO_{ads} in

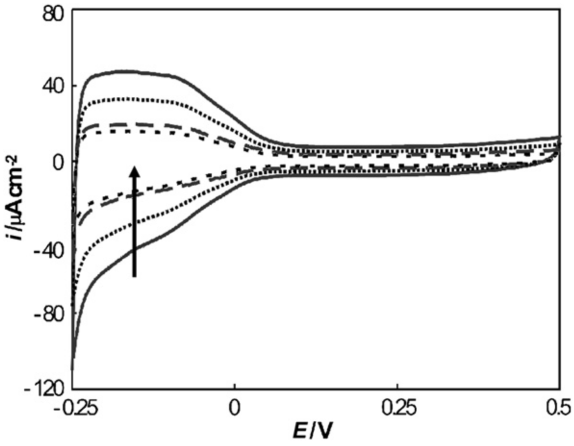

Fig. 3 – Cyclic voltammograms for Nafion/Pt–Ru/GC in 0.5 M H_2SO_4. Nafion® 117 film thickness: without ionomer (▬), 0.85 μm (•••••), 5.10 μm (▬ ▬), and 9.72 μm (■ ■). Sweep rate 50 mV s^{-1}.

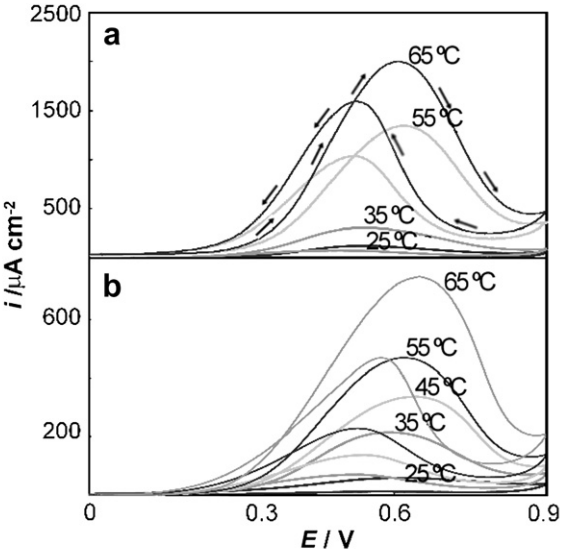

Fig. 4 – Cyclic voltammograms (tenth cycle) for Nafion/Pt–Ru/GC in 1 M CH_3OH/0.5 M H_2SO_4 (sweep rate 50 mV s^{-1}) at diverse temperatures for Nafion® 117 films of different thickness: 0.85 μm (a), 9.72 μm (b).

presence of OH_{ads} groups. The Tafel slope values agree with those determined by other author [4,10–12] that considered the step 4 as the rds.

$$CH_3OH + Pt \rightarrow Pt\text{-}CH_3OH_{ads} \quad (1)$$

$$Pt\text{-}CH_3OH_{ads} \rightarrow Pt\text{-}CO_{ads} + 4H^+ + 4e^- \quad (2)$$

$$H_2O + Ru \rightarrow Ru\text{-}OH_{ads} + H^+ + e^- \quad (3)$$

$$Pt\text{-}CO_{ads} + Ru\text{-}OH_{ads} \rightarrow Pt + Ru + CO_2 + H^+ + e^- \quad (4)$$

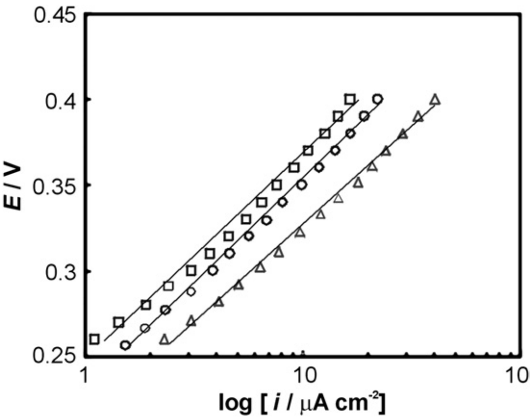

Fig. 5 – Tafel plot at 25 °C for Nafion/Pt–Ru/GC in 1 M CH_3OH/0.5 M H2SO_4 Nafion® films of different thickness: 0.85 μm (△), 5.10 μm (○), 9.72 μm (□).

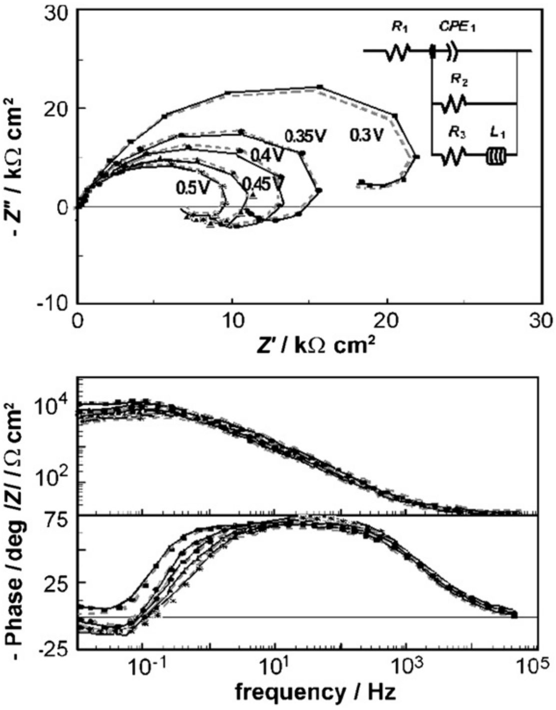

Fig. 6 – Nyquist and Bode plots for Nafion/Pt–Ru/GC electrodes in 1 M CH_3OH/0.5 M H_2SO_4 at 25 °Cs: Nafion® film thickness 5.10 μm. Solid lines represent the fitted data obtained with the equivalent circuit showed in the figure.

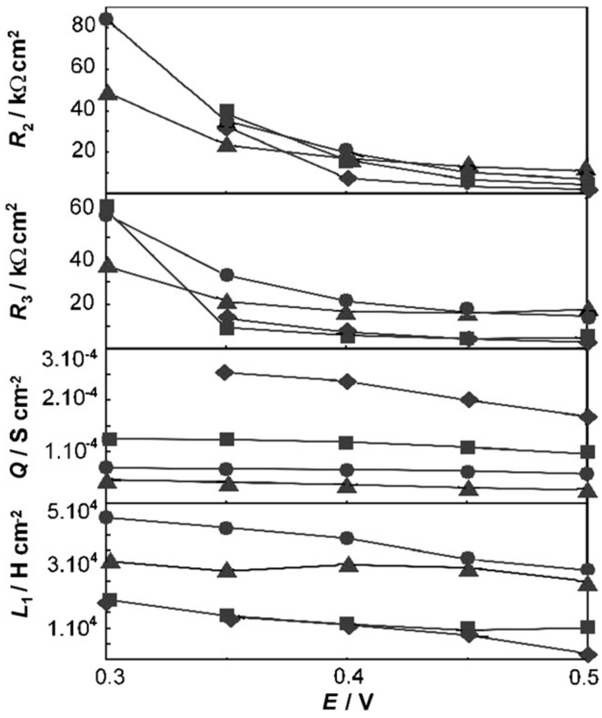

Fig. 7 – Physically significant parameters plotted as a function of the electrode potential. Data obtained from the fits of impedance spectra to the equivalent circuit in Fig. 6. Nafion® film thickness: without ionomer (◆), 0.85 μm (■), 5.10 μm (▲), 9.72 μm (●).

Table 2 – Steady state catalytic activities of methanol oxidation on electrodeposited bimetallic Pt–Ru/GC as synthesized in this work and some catalysts prepared by different deposition techniques.

Pt–Ru/C	at. % Ru	E/V	Substrate	Precursor	Deposition method/alcohol solution	i/μA cm^{-2}					
						25 °C	35 °C	45 °C	55 °C	60 °C	65 °C
Without Nafion®	25	0.3	GC	H_2PtCl_6, $RuCl_3$	See experimental section 1 M CH_3OH + 0.5 M H_2SO_4	71.6	174.6	220.1	342.7	–	490.9
0.85 μm						54.7	116.7	145.3	223.6	–	325.0
5.10 μm						29.4	71.5	85.4	111.8	–	141.7
9.72 μm						26.2	67.3	80.6	105.1	–	131.8
[20]	12	0.5	HOPG	K_2PtCl_6, $RuCl_3$	Cyclic voltammetry Sequential Pt and Ru deposition	52					
	10				Cyclic voltammetry. Simultaneous Pt and Ru deposition. 1 M CH_3OH + 0.5 M H_2SO_4	27					
[21]	40	0.25	Vulcan[d]	Non identified	Colloidal method. $NaHSO_3/H_2$ 2 M CH_3OH + 0.5 M H_2SO_4	28					
	40		Vulcan-O[a]			75					
	50		Carbon[b]			56					
[22]	41		Vulcan[d]	H_2PtCl_6, $RuCl_3$	Colloidal method. $NaHSO_3/H_2O_2/H_2$ 1 M CH_3OH + 0.5 M H_2SO_4	13					
	41		Vulcan-O			30.5					
	44		Vulcan-N[c]			24					
		0.3									
	44		Vulcan[d]		Impregnation method. i-PrOH.	14					
	44		Vulcan-O			12					
	41		Vulcan-N			16					
[23]		0.25	Carbon[d] black	$Pt(NH_3)_2(NO_2)_2$ + $Ru_3(CO)_{12}$	Coimpregnation method, EtOH/H2 Pyrolysis						
	50			$RuNO(NO_3)_x$	temperature 200 °C 1 M CH3OH + 0.5 M H2SO4					160	
	50									170	
[24]	48	0.4	Vulcan[d]	H_2PtCl_6, $RuCl_3$	Microemulsion method. Ciclohexane/HCHO/NP5 + NP9 2 M CH_3OH + 0.5 M H_2SO_4	74					

a Oxygen functionalized carbon material.
b HiSPEC 5000, Johnson & Matthey.
C Nitrogen functionalized carbon material.
d Carbon black and Vulcan XC-72 supported over GC.

To clarify the influence of the ionomer film on the electrode behavior EIS measurements were carry out. Fig. 6 shows impedance spectra of a Nafion/Pt–Ru/GC electrode at room temperature for methanol oxidation. The Nyquist plots show a capacitive semicircle that appears in the first quadrant and a semicircle that appears in the fourth quadrant indicating inductive behavior. A reduction in the 'diameter' of the capacitive loop with increasing electrode potential indicates that the charge-transfer resistance for methanol oxidation becomes smaller.

The phase angle Bode plots show a broad maximum composed by two poorly defined peaks. The first one it seems to be unrelated to kinetics, and may be associated with the existence of a constant phase element (CPE) that distorts the electrode response. At lower frequencies, a second maximum can be seen that decreases and moves to higher frequencies when the potential is raised. At frequencies lower than 0.1 Hz, a negative maximum appears that shifts to higher frequencies when the potential is increased. This behavior can be ascribed to the existence of two different time constants, the one at high frequencies corresponding to a fast reaction step (methanol dehydrogenation process) and the other at low frequencies corresponding to a slow reaction step (oxidative desorption reaction of CO_{ads} molecules).

In the equivalent circuit, R_1 represents the sum of the electrolyte and the ionomer film resistance and R_2 is the charge-transfer resistance associated with methanol oxidation. R_3 and L_1 are associated with the adsorption and oxidation of intermediates formed in the reaction, whereas the double layer capacitance has been represented by a constant phase element CPE_1.

R_2, R_3 and L_1 decrease when the electrode potential is increased from 0.3 to 0.5 V, while Q_1 remains almost constant (Fig. 7). Between 0.3 V and 0.4 V the value of R_2 fall abruptly, then the diminution with the potential becomes less important. The same behavior is observed in R_3 values, but in this case, the gradual decrease is associated with an increase of the oxidation rate of the intermediaries with the potential [13]. L_1 is an indicator of the amount of CO_{ads} on the catalyst surface. The amount of CO_{ads} increases as this species cannot be effectively oxidized to CO_2 at a lower potential (i.e., 0.3 V); therefore, L_1 exhibits a larger value. When the potential increases to a higher value, e.g., 0.5 V, the CO_{ads} is efficiently oxidized to CO_2, so the amount of adsorbed intermediary decreases and L_1 exhibits a smaller value as shown in Fig. 6.

From Fig. 7 it can be seen that R_1 is only slightly influenced by the ionomer film thickness, but in the case of the other fitted parameters, (Q_1, R_2, R_3 and L_1) stronger influence is observed. Q_1 decreases when there is a film of Nafion on the electrodes, and this may be considered indicative of a reduction of the active surface area. On the other hand, the values of the parameters R_2, R_3 and L_1 increase when the polymeric film becomes thicker. These changes probably are associated with the partial blockage of the surface active sites that difficult the methanol oxidation reaction, and also carbon dioxide bubbles presence in the Nafion® channels can exert an adverse influence on the catalyst behavior. The increases in R_2, R_3 and L_1 become less pronounced than expected with the thicker Nafion layer. This behavior can be associated with a comparable quantity of available active sites for methanol oxidation and with the formation of bigger clusters of water inside the hydrophilic domains of the ionomer in the thickest film.

EIS results suggest that CO is the only "kinetically significant" adsorbed intermediate. However, there is general agreement that methanol oxidation to CO_2 involves the presence of OH_{ads} on Ru atoms. Melnick et al. [14] and Otomo et al. [15] suggested that other species must be present on the catalyst surface, even when they proposed single-adsorbed equivalent circuits. On the other hand, Hsing et al. [16] described their impedance data in terms of a model that consider the presence of two adsorbates (CO and OH). Notwithstanding, they found that the impedance spectra show only two arcs as would occur for a single-adsorbate mechanism. It is possible that CO_{ads} and OH_{ads} formation and consumption are coupled and hence both species are indistinguishable by this technique [17].

3.3. *Catalytic activity evaluation*

The electrocatalytic behavior of the electrodes prepared in this work was evaluated by potentiostatic experiments in the potential region that is relevant for methanol oxidation in DMFC, and compared with some data available in the literature (Table 2). The catalytic activity at different temperatures for the electrodes prepared here, even those that contain the polymeric film with different thicknesses, are relatively good when are compared with those prepared by other electrochemical techniques [18,19], colloids formation [20,21], impregnation [21,22] and microemulsion methods [23]. The better performance of the catalysts presented in this work can be associated with their pronounced defective structure, i.e. high concentration of intergrain boundaries and nanopores [23]. These discontinuities in the crystal planes may act similarly to low coordinated sites (steps and kinks) on single crystalline and other extended surfaces [24], which exhibit very high catalytic activity for methanol oxidation. In addition, homogeneity in mixing the two metals at the atomic scale [25], the ruthenium content in the solid solution and differences in the crystalline structure of the deposits are expected to be very important reasons. Moreover, the presence of functional groups can contribute to improve electrode performance, since the presence of oxygenated functional groups strongly affects the behavior of Pt–Ru catalyst [26].

4. Conclusions

The electrodes prepared by successive cycles of potentiostat pulses, present a good activity in methanol oxidation, even when a polymeric film is deposited over the catalyst.

The different electrochemical experiments show a decrease of the activity in the Nafion/Pt–Ru/GC electrodes with respect to the Pt–Ru/GC electrode as a consequence of the partial blocking of the surface active sites by the hydrophobic domains of the polymeric film and the retarding of CO_2 removal from the active platinum sites by the polymer making difficult CH_3OH diffusion toward the electrode surface.

EIS results indicated that the presence of the ionomer does not affect the mechanism of the methanol oxidation reaction.

Methanol electro-oxidation proceeds with formation of at least two adsorbed intermediaries that participates in the rds, although both species are indistinguishable by EIS, indicating that their formation and consumption are coupled.

Acknowledgements

This work was supported by ANPCYT grant No 10-11133, UNS grant 24/M097 and CIC. J.M.S. is grateful to the CONICET for a postdoctoral fellowship.

REFERENCES

[1] Wei ZD, Chan SH. Electrochemical deposition of PtRu on an uncatalyzed carbon electrode for methanol electrooxidation. Journal of Electroanalytical Chemistry 2004;569:23–33.

[2] Iwasita T. In: Vielstich W, Gasteiger HA, Lamm A, editors. Handbook of Fuel cells fundamentals, technology and applications, vol. 2. New York: John Wiley & Sons; 2003.

[3] Sone Y, Ekdunge P, Simonsson D. Proton conductivity of Nafion 117 as measured by a four-electrode AC impedance method. Journal of the Electrochemical Society 1996;143: 1254–9.

[4] Sieben JM, Duarte MME, Mayer CE. Supported Pt and Pt–Ru catalyst prepared by potentiostatic electrodeposition for methanol electrooxidation. Journal of Applied Electrochemistry 2008;38:483–90.

[5] Bard AJ, Faulkner CR. Electrochemical methods, fundamentals and applications. 2nd ed. Singapore: Wiley & Sons Inc.; 1980.

[6] Plyasova LM, Yu Molina I, Gavrilov AN, Cherepanova SV, Cherstiouk OV, Rudina NA, et al. Electrodeposited platinum revisited: tuning nanostructure via the deposition potential. Electrochimica Acta 2006;51:4477–88.

[7] Gloaguen F, Léger J-M, Lamy C, Marmann A, Stimming U, Vogel R. Platinum electrodeposition on graphite: electrochemical study and STM imaging. Electrochimica Acta 1999;44:1805–16.

[8] Jiang J, Kucernak A. Investigations of fuel cell reactions at the composite microelectrode|solid polymer electrolyte interface. I. Hydrogen oxidation at the nanostructured Pt|Nafion® membrane interface. Journal of Electroanalytical Chemistry 2004;567:123–37.

[9] Vidaković T, Christov M, Sundmacher K. Rate expression for electrochemical oxidation of methanol on a direct methanol fuel cell anode. Journal of Electroanalytical Chemistry 2005; 580:105–21.

[10] Vidaković T, Christov M, Sundmacher K. Investigation of electrochemical oxidation of methanol in a cyclone flow cell. Electrochimica Acta 2004;49:2179–87.

[11] Zecevic SK, Wainright JS, Litt MH, Gojkovic SLj, Savinell RF. Kinetics of O_2 reduction on a Pt electrode covered with a thin film of solid polymer electrolyte. Journal of the Electrochemical Society 1997;144:2973–82.

[12] Gasteiger HA, Markovic N, Ross PN, Cairns E. Temperature-dependent methanol electro-oxidation on well-characterized Pt–Ru alloys. Journal of the Electrochemical Society 1994;141:1795–803.

[13] Seiler T, Savinova ER, Friedrich KA, Stimming U. Poisoning of PtRu/C catalysts in the anode of a direct methanol fuel cell: a DEMS study. Electrochimica Acta 2004;49:3927–36.

[14] Melnick RE, Palmore GTR. Impedance spectroscopy of the electro-oxidation of methanol on polished polycrystalline platinum. Journal of Physical Chemistry B 2001;105: 1012–25.

[15] Otomo J, Li X, Kobayashi T, Wen Ch, Nagamoto H, Takahashi H. AC-impedance spectroscopy of anodic reactions with adsorbed intermediates: electro-oxidations of 2-propanol and methanol on carbon-supported Pt catalyst. Journal of Electroanalytical Chemistry 2004;573:99–109.

[16] Hsing I-M, Wang X, Leng Y-J. Electrochemical impedance studies of methanol electro-oxidation on Pt/C thin film electrode. Journal of the Electrochemical Society 2002;149: A615–21.

[17] Seland F, Tunold R, Harrington DA. Impedance study of methanol oxidation on platinum electrodes. Electrochimica Acta 2006;51:3827–40.

[18] Rodríguez-Nieto FJ, Morante-Catacora TY, Cabrera CR. Sequential and simultaneous electrodeposition of Pt–Ru electrocatalysts on a HOPG substrate and the electro-oxidation of methanol in aqueous sulfuric acid. Journal of Electroanalytical Chemistry 2004;571:15–26.

[19] Gómez de la Fuente JL, Martínez-Huerta MV, Rojas S, Terreros P, Fierro JLG, Peña MA. Enhanced methanol electrooxidation activity of PtRu nanoparticles supported on H_2O_2-functionalized carbon black. Carbon 2005;43:3002–5.

[20] Gómez de la Fuente JL, Martínez-Huerta MV, Rojas S, Terreros P, Fierro JLG, Peña MA. Methanol electrooxidation on PtRu nanoparticles supported on functionalised carbon black. Catalysis Today 2006;116:422–32.

[21] Takasu Y, Fujiwara T, Murakami Y, Sasaki K, Oguri M, Asaki T, et al. Effect of structure of carbon-supported PtRu electrocatalysts on the electrochemical oxidation of methanol. Journal of the Electrochemical Society 2000;147: 4421–7.

[22] Liu Z, Ling XY, Lee JY, Su X, Gan LM. Nanosized Pt and PtRu colloids as precursors for direct methanol fuel cell catalysts. Journal of Materials Chemistry 2003;13:3049–52.

[23] Hoster HE, Bergbreiter A, Erne PM, Hager T, Rauscher H, Behm RJ. PtxRu1-x/Ru(0001) surface alloys-formation and atom distribution. Physical Chemistry Chemical Physics 2008;10:3812–23.

[24] Gavrilov AN, Savinova ER, Simonov PA, Zaikovskii VI, Cherepanova SV, Tsirlina GA, et al. On the influence of the metal loading on the structure of carbon-supported PtRu catalysts and their electrocatalytic activities in CO and methanol electrooxidation. Physical Chemistry Chemical Physics 2007;9:5476–89.

[25] Gasteiger HA, Marković N, Ross Jr PN, Cairns E. Methanol electrooxidation on well-characterized platinum–ruthenium bulk alloys. Journal of Physical Chemistry 1994;97:12020–9.

[26] Petrii OA. Pt–Ru electrocatalysts for fuel cells: a representative review. Journal of Solid State Electrochemistry 2008;12:609–42.